Analysis of a transformer designed for wireless power transmission system for different distance and alignment conditions and optimization with a developed algorithm

Y. Özüpak[a]*, M. Çınar[b]

[a]Silvan Vocational School, Dicle University, Diyarbakır, Turkey
[b]Tatvan Vocational School, Bitlis Eren University, Bitlis, Turkey
*Corresponding Author e-mail: yildirim.ozupak@dicle.edu.tr, +904122411000

KEYWORDS
WPT
Efficiency
FEM
Maxwell-3D
WHA

Abstract. In this study, the investigation of various positions of receiver and transmitter coils in a wireless power transfer (WPT) system was conducted using magnetic resonance-based coupling theory. The aim was to determine the air gap limits for achieving high efficiency in analyzing different coil positions. Self-inductance, mutual inductance, and coupling coefficient were calculated for this purpose. The efficiency of the system was determined for different coil positions by calculating input and output powers. Additionally, an optimized wireless power transfer system was achieved using the developed Wound Healing Algorithm (WHA). The MATLAB Simulink was employed to obtain mutual inductance and coupling coefficient values based on the distance between the coils in the wireless power system. The efficiency of the system was then calculated. The results were compared with those obtained from ANSYS Maxwell for interpretation. The findings indicated efficient power transfer up to specific distances in various coil positions. The points where efficiency started to decrease provided insights into determining the air gap and angular limits of the designed WPT system.

1. Introduction

While the wireless transmission of energy has been a subject of study for over two centuries, effectively implementing solutions within the electrical-electronic engineering culture remains a significant challenge. The journey, initiated by Nikola Tesla, has gained increasing importance with technological advancements, evolving into a multi-disciplinary field. Wireless energy transfer has become a shared focus across various disciplines. Furthermore, it plays a crucial role in realizing proposals like electric vehicles, home electronics, and medical applications, which are expected to see more widespread use in the future [1].

The studies on wireless power transfer, initiated by Nikola Tesla, can be broadly categorized into two main groups: near-field and far-field power transfer technologies. Far-field energy transfer involves the radiation of electromagnetic waves at high frequencies and is suitable for transferring energy over long distances. However, implementing far-field technology demands power electronic circuit technologies to operate at very high frequencies, making it both expensive and less efficient. On the other hand, near-field power transfer operates through inductive coupling at distances smaller than one wavelength and at low frequencies. This technology is comparatively more efficient and cost-effective, making it a preferred choice, especially in wireless charging applications. Numerous commercial products utilizing near-field power transfer are available, including electric toothbrushes, medical implants, mobile device chargers, and electric vehicle charging systems [2].

Until now, wireless energy transfer has been explored through various methods, including electromagnetic radiation, microwave techniques, laser beams, electromagnetic induction, and magnetic resonance coupling. The initial attempts at wireless power transmission through electromagnetic radiation can be traced back to Nikola Tesla. However, this project faced obstacles and remained incomplete after sponsors withdrew their support [3].

The concept of power transfer through microwaves gained traction with the development of high-power microwave transmitters post-World War II. William

Brown, a pioneer in this field, designed a model helicopter powered by microwave beams in 1964 [4]. Sahai and Graham achieved energy transfer using lasers, a form of wireless energy that operates with low efficiency over long distances. While laser radiation, commonly suited for space applications, poses significant risks such as harm to vision at low powers and potential harm to living organisms through partial heating at high powers [5].

Another explored method is electromagnetic induction technology, which demonstrated effective working at short distances (a few centimeters) with high efficiencies in a particular study. However, this method has limitations, including the need for close proximity and challenges in aligning the coils due to the short distance [6].

Magnetic resonance coupling theory represents a groundbreaking wireless energy transfer technology that originated in 2007 with the invention of WiTricity by MIT scientists. Utilizing this magnetic resonance coupling theory, they achieved wireless feeding of a 60 W lamp at a distance exceeding two meters with an efficiency of approximately 40%. This innovation enabled the wireless transmission of electrical energy for medium distances. The WiTricity system relies on magnetic resonance coupling for energy transmission, where, under ideal conditions, the energy in the primary coil is entirely transferred to the secondary coil. Consequently, efficient energy transfer occurs between resonant objects [7-10].

In recent years, magnetic resonance coupling studies have supplanted inductive power transmission systems based on magnetic induction theory due to their higher efficiency [11-13]. The alignment of transmitter and receiver coils in the wireless power transfer (WPT) system also significantly impacts efficiency [14]. Aligned coils can operate at higher air gaps with greater efficiency compared to angularly and positionally unaligned coils. Reference [15] conducted a study on estimating the coupling coefficient, highlighting that efficiency depends on factors such as the distance between coils, the environment, and their positions. The importance of estimating the coupling coefficient has been emphasized in efforts to enhance efficiency, with the estimation based on welding voltage, welding current, output voltage, and output current information.

Controllers designed using conventional techniques often exhibit poor performance and may not be suitable for optimally controlling bidirectional Inductive Power Transfer (IPT) systems. An alternative approach for optimizing parameters involves the use of gradient-free optimization methods such as genetic algorithms (GAs), evolutionary computation, particle swarm optimization, etc. [16, 17].

In reference [18], parallel-parallel compensation is implemented in a system utilizing the magnetic resonance wireless power transmission method. To stabilize the voltage on the load of the secondary circuit, a combined controller comprising a DC-controlled variable capacitor and a Proportional-Integral (PI) controller is proposed. The proposed controller maintains the output voltage at 5 V with a frequency of approximately 290 kHz, enabling power transmission between 5.7-7.6 Watts.

System parameters directly impact the efficiency of the system [19]. Therefore, optimizing a selected parameter in dynamic systems can bring the system efficiency back to its maximum level. System control can be applied to both the primary and secondary circuits. In single receiver systems, controlling the primary circuit is more appropriate, while in multi-receiver systems, control is typically applied to the secondary circuit. Various methods are employed for the control of wireless power transmission systems [20].

The values of k and M for Wireless Power Transfer (WPT) system represent the mutual inductance (M) and coupling coefficient (k) values of the wireless energy transfer system. These values provide information about the strength and efficiency of the electromagnetic coupling between the transmitting coil and the receiving coil. The coupling coefficient (k) is a measure of the electrical coupling between the two coils. It usually takes a value between 0 and 1 and the closer it is to 1, the stronger the coupling between the coils. Mutual inductance (M) is a measurement of how much influence the magnetic field of one coil has on the other coil. A higher mutual inductance indicates that the electromagnetic coupling between the coils is stronger. These values are important in designing and optimizing the WPT system. Optimum k and M values must be determined to ensure high efficiency and power transfer. These values are usually determined using simulation tools or mathematical calculations to analyze the electromagnetic characteristics of the design.

In this study, the efficiency of transformer models designed for Wireless Power Transfer (WPT) was investigated for different positions and air gap distances. Mutual inductance, resonance frequency, input and output currents were examined for various positions of the models and variable air gap distances. The equivalent circuit and coils of the magnetic resonance coupling system were obtained using different platforms of the ANSYS program. Subsequently, transient analysis of the WPT system was conducted for different positions of the receiver and transmitter coils. The program, created in the Matlab Simulink environment with the assistance of the developed wound healing algorithm, facilitated optimum calculations of parameters such as k, M, and efficiency based on distance. In this paper, various positions of the transmitter and receiver coils of a wireless energy transfer (WPT) system are investigated using magnetic resonance-based coupling theory. The aim is to determine the air gap limits for high efficiency by analyzing different coil positions. The wireless energy transfer system is optimized using the developed Wound Healing Algorithm (WHA). The results are compared with the results obtained from ANSYS Maxwell for interpretation.

2. Material and method

In this section of the study, the fundamental working principle of the equivalent circuit employed in the simulation is elucidated. The circuit depicted in Figure 1 represents the basic equivalent circuit of the Wireless Power Transfer (WPT) system. This circuit is instrumental in analytically calculating parameters such as input impedance, transmitted power, and efficiency [21, 22].

In this equivalent circuit, I_1 input current (emitter current), I_2 output current (receiver current), V_1 input voltage, R transmit and receive systems' internal resistances, C transmit and receive resonant capacitors, L_1 transmit coil, L_2 receive coil, L_m counter shows the inductance and Z_{load} load impedance (characteristic impedance). Eq. (1) shows the perimeter Eq. of the transmitter part. Eq. (2) shows the perimeter Eq. of the receiver part [13].

$$V_1 = I_1\left(R + jL_1\omega + \left(\frac{1}{j\omega C_1}\right)\right) - I_2\left(jL_m\omega\right) \quad (1)$$

$$0_1 = I_2\left(jL_2\omega + \left(\frac{1}{j\omega C_2}\right)\right) - I_2\left(jL_m\omega\right) \quad (2)$$

Using Eq. (1) and Eq. (2), the relationship between the currents of the receiver and transmitter coils is obtained as in Eq. (3).

$$I_2 = I_1\left(\frac{jL_m\omega}{jL_2\omega + \left(\frac{1}{j\omega C_2}\right) + RZ_0}\right) \quad (3)$$

If we substitute Eq. (1) in Eq. (3) and divide the resulting voltage Eq. by the input current, the equivalent impedance (input impedance) is obtained as in Eq. (4).

$$Z_{eq} = R + \frac{1}{j\omega C_1} + j\left(L_1 - L_2\right) + \left(\frac{1}{jL_m\omega} + \frac{1}{j\left(L_2 - L_m\right)\omega + \frac{1}{j\omega C_2} + Z_0 + R}\right) \quad (4)$$

The equivalent circuit in Figure 1 can also be represented by the T-type equivalent circuit as in Figure 2 [23].

The efficiency of this system is expressed as in Eq. (5).

$$\eta = \frac{P_o}{P_i} = \frac{I_o^2 Z_o}{I_i^2 Z_i} \quad (5)$$

Where, the current I_o is equal to the current through the receiver I_2, the input current is equal to the current through the emitter I_1, the impedance Z_o is equal to the impedance Z_{load}. If we write Eq. (3) as the ratio of output current to input current, Eq. (6) is obtained.

$$\frac{I_o}{I_i} = \frac{jL_m\omega}{jL_2\omega + \frac{1}{j\omega C_2} + R + Z_o} \quad (6)$$

When Eq. (6) and Eq. (4) are placed in Eq. (5), the yield Eq. is obtained as in Eq. (7).

$$\eta = \left[\frac{jL_m\omega}{jL_2\omega + \frac{1}{j\omega C} + Z_o + R_2} \right]^2 x \frac{Z_o}{\left(R + jL_1\omega + \frac{1}{j\omega C} + \frac{L_m^2\omega^2}{jL_2\omega + \frac{1}{j\omega C} + Z_0 + R_2} \right)} \quad (7)$$

Eq. (7) establishes conditions for maximum efficiency, where (Lm) represents the opposite inductance, (L) denotes the receive and transmit inductance, (Z0) stands for the characteristic impedance, and (R) represents internal resistance. Eq. (8) further delineates the limit determining the occurrence of either a double or single resonance frequency for this system.

$$L_m^2 = \frac{Z_o^2 - R^2}{\omega_o^2} \quad (8)$$

2.1 Developed algorithm (Wound Healing Algorithm)

The clonal selection algorithm is an algorithm that leverages the characteristics of the immune system's response when a foreign substance enters the body. In the context of wound healing, a novel algorithm based on the clonal selection principle has been developed [24]. The results obtained from this clonal selection algorithm have been compared with the outcomes generated by a widely used program, such as ANSYS. This comparison likely serves to validate and assess the efficacy of the newly developed algorithm in the context of wound healing.

$$Nc = \sum_{i=1}^{n} round\left(\frac{N}{i}\right) \quad (9)$$

N_c: Clone numbers that produced from each antigen
N: Solution population's total number
n: Selected antibodies number

The wound healing algorithm is grounded in the clonal selection principle. Eq. (1) is utilized to calculate the number of clones generated. The wound healing formula, introduced with additional parameters α (cloning) and f (cloning acceleration factor) in Eq. (9), yields the final state as expressed in Eq. (12). Through the adjustment of these new parameters, numerous optimized results are explored. The flow chart of the developed wound healing algorithm is illustrated in Figure 3. In the initialization of the population P, the selection process begins by choosing antibodies with the most effective immunologic response (affinity) value to form the new Pn population, following a fundamental rule. Throughout the selection process, the emphasis is on the affinity value of antibodies. Subsequently, individuals in the population are cloned, and new populations are created. The number of clones varies based on the affinity value. In this phase, a new population is formed by applying hypermutation to the clones. The hypermutation process is inversely proportional to the affinity value, meaning that antibodies with high affinity have a low mutation rate, while those with low affinity have a higher mutation rate. Consequently, antibodies deviating from the optimal solution undergo more mutation processes. Following the hypermutation, among the obtained clones, those with a low similarity ratio are replaced with new ones. Ultimately, the optimal results are achieved through the interplay of selection, cloning, and mutation processes in the developed wound healing algorithm.

2.2. Solution stages of wound healing algorithm

- Use N antibodies to generate the initial population (P).
- Determine the affinity of each antibody in the P population. Select the n antibody (N) with the highest affinity to generate a P_n population. To measure the affinity value between an antibody and an antigen, the distance between them is usually taken into account. This is calculated using Eq. (10) and the Euclidean distance Eq..

$$d = \sum_{i=1}^{N} (Ag_i - Ab_i)^2 \quad (10)$$

The calculated d is compared with the threshold value λ and the marking error E is calculated as in Eq. (11):

$$E = d - \lambda \quad (11)$$

- Clone the n antibodies selected in step 2 and construct N_c using Eq. (12).

$$Nc_i = \sum_{i=1}^{n} round\left(\frac{\alpha * N_s * f}{i}\right) \quad (12)$$

α : Cloning factor (value range is 0 to 1)

f: Cloning acceleration factor (value range is 0.9 to 0.99)

N_s: The best number of antibodies selected in step 2

- Mutate the N_c clone population. Create this subpopulation. Calculate the affinity value for each antibody from the subpopulation, choose the antibody with the best value and add it to the starting population.
- Replace the low-affinity antibody with new antibodies. If population value *P* is less than *N*, generate antibodies to complete the population.

Wound healing algorithm used the parameters and values in the Table 1 while calculating the optimum values. Since the algorithm is a stochastic algorithm, the initial values are randomly assigned. The program continues to run until the convergence test is performed.

2.3 Design of rectangular WPT transformer model

In this part of the study, the design of rectangular WPT transformers with ANSYS-Maxwell program is emphasized. The rectangular coils given in Figures 4. The dimensions of the rectangular transformer model are presented in Table 2.

In the magnetic resonance-coupled Wireless Power Transfer (WPT) system, the model features primary and secondary winding numbers identical to the circular transformer model. For each specified air gap, both aligned and unaligned states have been designed. The circuit representations of the receiver and transmitter windings were established by modeling the circuit in the ANSYS-Maxwell Circuit Editor program.

Additionally, in the ANSYS-Maxwell-3D program, various positions of the transmitter and receiver coils were generated, as illustrated in Figure 4. Unaligned transformers are specifically depicted in Figure 5. This comprehensive approach allows for a thorough examination of the system's behavior under different configurations and air gap distances.

The designed wireless power transfer transformers utilize Litz conductors, and analyses were conducted under various location and distance conditions for these transformers. Litz wire, derived from the German word "Litzendraht," meaning woven wire, is a wire group composed of multiple insulated (enamel-coated) conductor wires twisted or braided around each other, or partially braided between each other. To grasp the purpose of Litz wire, it's essential to discuss the skin effect. In a conductor carrying direct current, the current uniformly distributes throughout the material cross-section. However, when alternating current flows through the same conductor, the presence of eddy currents caused by frequency disrupts this uniformity, and the current starts to flow closer to the conductor surface. This phenomenon is known as the skin effect. As the frequency increases, the skin effect intensifies, and the depth of penetration decreases. Litz wire was developed to address this issue in high-frequency AC transmissions. Instead of using a single wire, the surface area is increased by forming multiple electrically identical paths through the re-twisting of a much lower insulated wire around itself. Litz wire is employed in high-frequency applications up to 1MHz to mitigate skin effect losses. These applications span a range of technologies, including high-frequency inductors, transformers, inverters, communications and ultrasonic/sonar equipment, TV and radio equipment, and induction heating equipment. Moreover, Litz wire finds application in wireless charging and inductive chargers.

3. Results and discussion

3.1 Analysis of aligned WPT transformers

The simulation results for the models are presented in Tables 3, 4, and 5. Notably, it is observed that the

alteration in the self-inductance of the coils is less pronounced compared to the change in the mutual inductance (M), indicating a higher sensitivity of M to variations in air gap distance and model positions. Specifically, the common inductance M and coupling coefficient k demonstrated an increase when the air gap distance between the transmit coil and the receiver coil decreased under different positional scenarios. This suggests that changes in the air gap distance have a more significant impact on mutual inductance and coupling coefficient, emphasizing the sensitivity of these parameters to variations in the physical configuration of the system.

The interface of the program developed in MATLAB is shown in Figure 6. An example calculation was made with the help of the program. In case of 2 cm distance and aligned coils *k*, *M* and efficiency calculation are seen.

The results obtained from the developed algorithm are presented in Table 6 alongside the results from the ANSYS program. Notably, when examining Table 6, it is observed that the efficiency calculation of the system is slightly higher with the wound healing algorithm. This can be attributed to the algorithm's iterative nature, where initial values are randomly assigned, and the program runs repeatedly until the convergence test is satisfied. In certain cases, the program is run at least 30 times, while in others, it runs at least 100 times to obtain the optimum value. The larger the mutual inductance (M) and coupling coefficient (k) values, the higher the power transmitted to the receiving coil. With the presence of a ferrite core in the design, the common inductance (M) and coupling coefficient (k) values were higher than those of the coreless transformer. The ferrite core condenses the generated magnetic field, maintaining it between the two coils, thus enabling higher M and k values. The variation in the intensity (B) of the built-in magnetic field for the different transformer design types is depicted in Figures 7, 8, and 9. These figures likely illustrate how the magnetic field intensity changes across the specified designs, providing valuable insights into the performance of the system. The color representation in the figures, where red indicates high magnetic flux and blue signifies the regions with the lowest flux density, offers a visual depiction of the magnetic field distribution. The transition from blue to red represents an increase in flux density. Specifically, when analyzing aligned Wireless Power Transfer (WPT) transformers, the alteration in the vertical distance between the coils was considered while maintaining a constant horizontal position between the coils. Notably, it was observed that the common inductance and coupling factor exhibited significant changes as the distance between the coils increased. This visual representation aids in understanding how adjustments in the physical configuration impact the magnetic field distribution and, consequently, the system's inductance and coupling characteristics.

3.2 Analysis of unaligned WPT transformers

In this part of the study, unaligned state analyzes of different transformer models designed for the WPT system were performed. The obtained values are presented in Tables 7-10.

In the analysis of unaligned Wireless Power Transfer (WPT) transformers, changes were made only in the horizontal positions while keeping the vertical distance between the coils constant. Interestingly, it was observed that the common inductance and coupling factor did not exhibit significant changes under these conditions. This indicates that variations in the horizontal positions of the coils, while maintaining a constant vertical distance, have a relatively minor impact on the common inductance and coupling factor.

Understanding these nuances in the behavior of the system components is crucial for optimizing the design and performance of wireless power transfer systems under different spatial configurations.

4. Conclusion

In this study, the impact of the alignment and misalignment states of the designed transformer models for the Wireless Power Transfer (WPT) system on the system's efficiency was examined, specifically when operating with the magnetic resonance coupling system. The simulation studies revealed that wirelessly transmitted electrical power achieves high efficiency in the 0-6 cm range, and efficiency rapidly decreases as the air gap distance increases beyond this threshold. In the unaligned state, a significant reduction in efficiency was observed due to the very low mutual common inductance value. However, it was noted that highly efficient wireless energy transfer could be achieved without alignment up to certain air gap values. The study conducted using ANSYS-Maxwell-3D took into account the skin effect and proximity effect on the transmitter and receiver coils of the wireless energy transfer system while calculating the efficiency value. Litz cable was employed in the design, and analyses were performed accordingly. The results obtained with the developed wound healing algorithm were compared with the ANSYS program in Tables 6 and 10. The outcomes indicate that the algorithm is superior, providing successful and accurate results, particularly in the context of wireless power transfer.

Acknowledgment

This work was carried out with commercial program Ansys Electronic 22.0. This project was supported by Dicle University Scientific Research Project Unit.

References

1. Yuki, T. Hikaru, H. Kazuki, K. et al., "Self-synchronized interference avoidance method for far-field wpt system," IEEE Wireless Power Technology Conference and Expo (WPTCE), San Diego, CA, USA, (2023), pp. 1-6, doi: 10.1109/WPTCE56855.2023.10215563.
2. Khan, S. M. and Bailey, C. "Design of chiral 4-tiered wireless power transfer (wpt) systems for vertiports," *2023 International Applied Computational Electromagnetics Society Symposium (ACES)*, Monterey/Seaside, CA, USA, (2023), pp. 1-2, doi: 10.23919/ACES57841.2023.10114746.
3. Wu, J. Deng, Y. and Shu, Z. "A no communication wpt system with dual resonant tank based on fundamental and harmonic current," *2023 IEEE 14th International Symposium on Power Electronics for Distributed Generation Systems (PEDG)*, Shanghai, China, (2023), pp. 439-444, doi: 10.1109/PEDG56097.2023.10215300.
4. Zaho, J. "A contrastive studies between magnetic coupling resonance and electromagnetic induction in wireless energy transmission", Electromagnetic Field Problems and Applications (ICEF),1-4. (2022)
5. Hong, X. Zhang, W. Xia, at all. "Loss characteristics of magnetic resonant wpt system with s-s topology," *2023 International Conference on Data Science and Network Security (ICDSNS)*, Tiptur, India, (2023), pp. 01-06, doi: 10.1109/ICDSNS58469.2023.10245311.
6. Bouanou, T. Fadil, E. Lassioui, at al. "Design methodology and circuit analysis of wireless power transfer systems applied to electric vehicles wireless chargers". *World Electr. Veh. J.* (2023(, *14*, 117. https://doi.org/10.3390/wevj14050117.
7. Su, G. J. Mohammad, M. and Galigekere, V. P. "Interoperability between three-phase and single-phase wpt systems," *2023 IEEE Wireless Power Technology Conference and Expo (WPTCE)*, San Diego, CA, USA, (2023), pp. 1-6, doi: 10.1109/WPTCE56855.2023.10215837.
8. Yamada, Y. and Imura, T. "An efficiency optimization method of static wireless power transfer coreless coils for electric vehicles in the 85 khz band using numerical analysis," IEEJ,

Transactions on Electrical and Electronic Engineering, Vol.17 No.10, (2022).
9. Yamada, Y. Sasaki, K. Imura, T. at all. "Design method of coils for dynamic wireless power transfer considering average transmission power and installation rate," IEEE 6th Southern Power Electronics Conference (SPEC 2021), Kigali Rwanda, (2021).
10. Fatih, I. Orhan, K. "Impedance analysis and variable capacity array application for wireless energy-transfer system via coupled magnetic resonances" GU J Sci, Part C, 8(4): 1005-1020, (2020).
11. Navid, R. Jun, W. and Xibo, Y. "In-situ measurement and investigation of winding loss in high-frequency cored transformers under large-signal condition". IEEE open journal Industry Applications, Vol. 3. (2022).
12. Feng, L. Yanjie, L. Siqi, Z. at all. "Wireless power transfer tuning model of electric vehicles with pavement materials as transmission media for energy conservation". Applied Energy 323 119631, (2022).
13. Aslan, E. Arserim, M. and Uçar, A. "A development of push-recovery control system for humanoid robots using deep reinforcement learning", Ain Shams Engineering Journal, Volume 14,Issue 10,102167, ISSN 2090-4479,https://doi.org/10.1016/j.asej.2023.10216. (2023)
14. Özüpak, Y. and Aslan, E. "Researching inductive power transfer for next generation electric vehicles". Ejons International Journal, 7(2), 220–232. (2023) https://doi.org/10.5281/zenodo.8265795.
15. Jeong, S. "Analysis of repetitive bending on flexible wireless power transfer (wpt) pcb coils for flexible wearable devices" in *IEEE Transactions on Components, Packaging and Manufacturing Technology*, (2022), doi: 10.1109/TCPMT.2022.3217291.
16. Passino, K. M. "Biomimicry for optimization, control, and automation". London, UK: Springer, (2004).
17. Chang, M. Ma, X. Han, J. at all. "Metamaterial adaptive frequency switch rectifier circuit for wireless power transfer system," in *IEEE Transactions on Industrial Electronics* (2022) doi: 10.1109/TIE.2022.3220908.
18. He, X. Zhu, C. Tao, J. at all. "Analysis and design of a cost-effective wpt system with single-input and multioutput based on buck-integrated rectifier," in *IEEE Transactions on Power Electronics*, vol. 38, no. 10, pp. 12388-12393, Oct. (2023), doi: 10.1109/TPEL.2023.3297712.
19. Hong, W. Lee, S. and Lee, H. "Sensorless control of series-series tuned inductive power transfer system" in *IEEE Transactions on Industrial Electronics*, (2022) doi: 10.1109/TIE.2022.3220885.
20. Wei, X. Qi, C. and Shou, L., "An optimized design of an electric vehicle wireless charging coupling coil" , 4th International Conference on Mechanical, Electrical and Material Application (MEMA 2021) 29-31 October (2021), Chongqing, China.
21. Singh, R. Sanjeevikumar, P. Kumar, at all. "Cable based and wireless charging systems for electric vehicles: technology and control, management and grid integration" Institution of Engineering and Technology, (2021).
22. Çiçek, M. Balcı, S. and Sabancı, K. "A comparative performance analysis of wireless power transfer with parametric simulation approach", Kastamonu University Journal of Engineering and Sciences, vol. 9, no. 1, pp. 17-32, Jun. (2023), doi:10.55385/kastamonujes.1298700.
23. Imura, T. and Hori, Y. "Maximizing air gap and efficiency of magnetic resonant coupling for wireless power transfer using equivalent circuit and neumann formula", IEEE Trans. Ind. Electron., 58, 4746-4752. (2011).
24. Çınar, M. "Optimal tuning of a PID controller using a wound healing algorithm based on the clonal selection principle". Transactions of the Institute of Measurement and Control. (2022);44(9):1770-1776. doi:10.1177/01423312211064658.

Figures

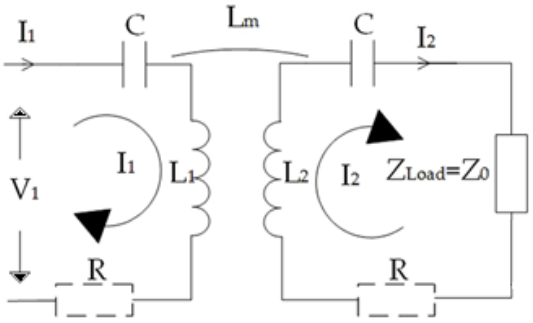

Figure 1. Equivalent circuit of wireless power transmission system

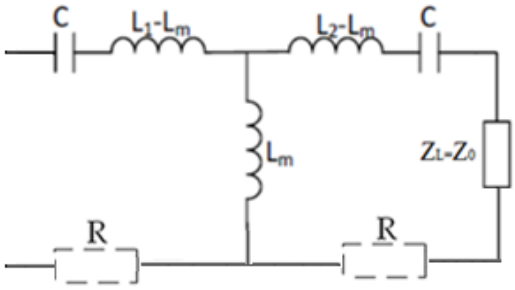

Figure 2. WPT system equivalent circuit

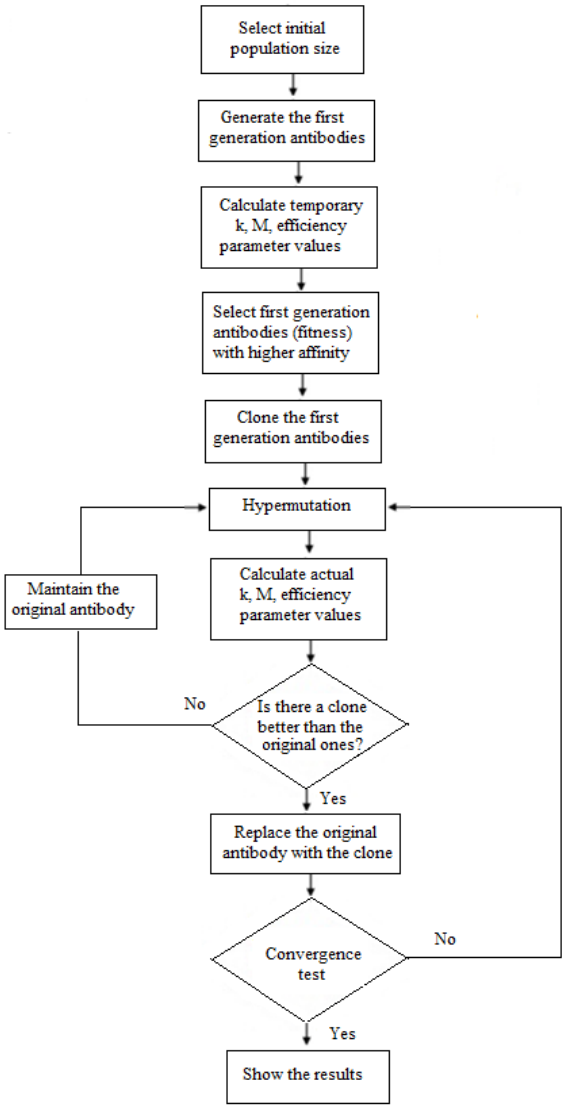

Figure 3. Wound healing algorithm flowchart

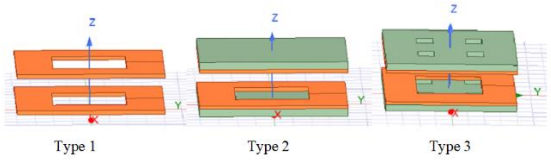

Figure 4. Aligned receiver and transmitter WPT models

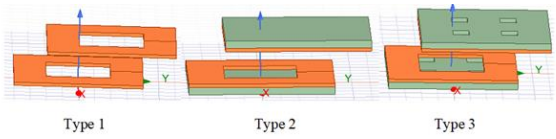

Figure 5. Unaligned receiver and transmitter WPT models

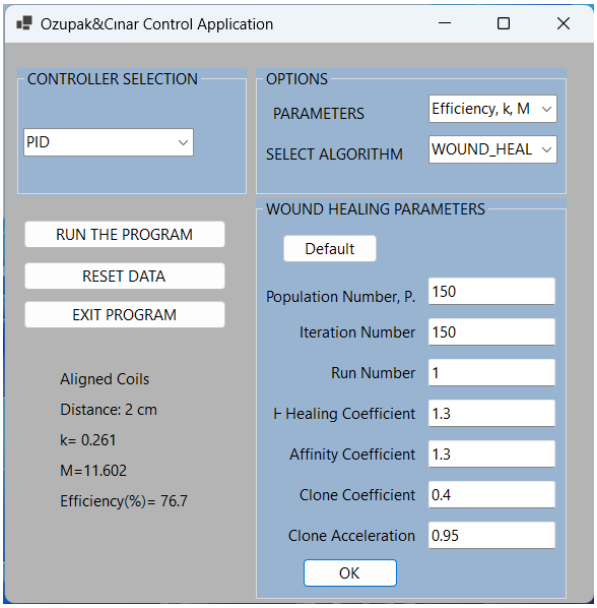

Figure 6. With the help of the developed program, sample k, M and efficiency calculation values

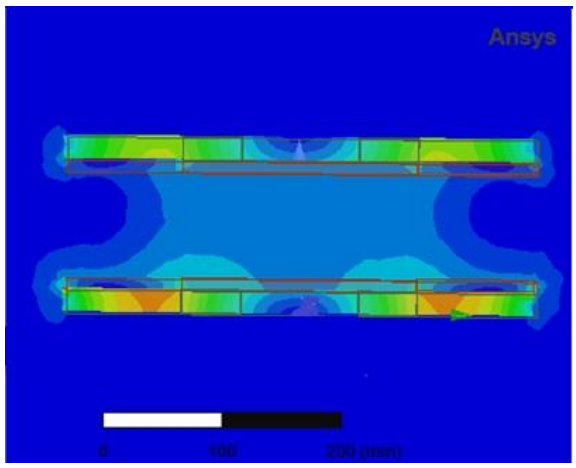

Figure 7. Magnetic flux distribution of Type 1 transformer

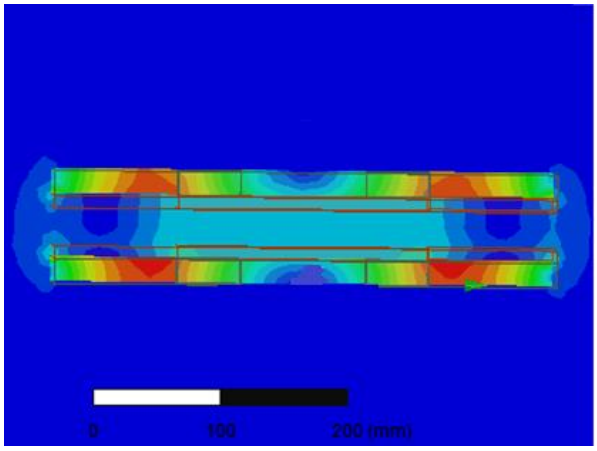

Figure 8. Magnetic flux distribution of Type 2 transformer

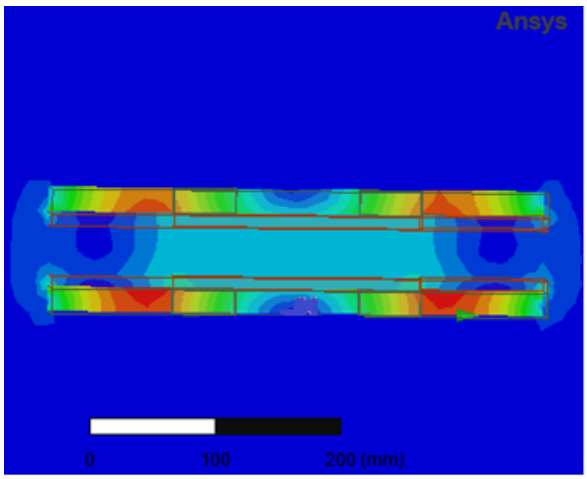

Figure 9. Magnetic flux distribution of Type 3 transformer

Tables

Table 1. Wound healing algorithm parameters and values

Parameter	Value
Population number	150
Iteration number	150
Run number	30
Healing coefficient	1.3
Affinity coefficient	1.3
Clone coefficient (α)	0.4
Clone acceleration (f)	0.95

Table 2- Dimensions of rectangular WPT transformer

Parameter	Receiver coil	Transmitter coil
Turn Number	24	42
Material thickness	2 mm	2 mm
Coil dimension	(395x395) mm	(395x395) mm
Core dimension	(398x398) mm	(398x398) mm
Aluminum plate dimension	(400x400) mm	(400x400) mm

Table 3-Analysis results of aligned coils of Type 1 WPT transformer

Distance	Coupling coefficient (k)	Transmitter coil inductance (L_p)	Receiver coil inductance (L_s)	Mutual inductance (M)	Efficiency (%)
0 cm	0.300	78.216 (μH)	25.545 (μH)	13.441 (μH)	80.4
2 cm	0.253	79.961 (μH)	26.112 (μH)	11.562 (μH)	76.1
4 cm	0.214	80.980 (μH)	26.457 (μH)	9.911 (μH)	70.9
6 cm	0.182	81.668 (μH)	26.701 (μH)	8.502 (μH)	51.3
8 cm	0.154	82.209 (μH)	26.842 (μH)	7.301 (μH)	39.2
10 cm	0.133	82.563 (μH)	26.959 (μH)	6.286 (μH)	24.5

Table 4- Analysis results of aligned coils of Type 2 WPT transformer

Distance	Coupling coefficient (k)	Transmitter coil inductance (L_p)	Receiver coil inductance (L_s)	Mutual inductance (M)	Efficiency (%)
0 cm	0.469	150.343 (μH)	49.105 (μH)	38.654 (μH)	88.3
2 cm	0.384	146.370 (μH)	47.763 (μH)	31.178 (μH)	84.2
4 cm	0.312	143.962 (μH)	47.012 (μH)	25.340 (μH)	73.1
6 cm	0.269	142.489 (μH)	46.505 (μH)	20.881 (μH)	59.6
8 cm	0.218	141.599 (μH)	46.229 (μH)	17.352 (μH)	45.2
10 cm	0.181	140.989 (μH)	45.948 (μH)	14.515 (μH)	31.8

Table 5- Analysis results of aligned coils of Type 3 WPT transformer

Distance	Coupling coefficient (k)	Transmitter coil inductance (L_p)	Receiver coil inductance (L_s)	Mutual inductance (M)	Efficiency (%)
0 cm	0.448	149.575 (μH)	48.702 (μH)	38.266 (μH)	86.3
2 cm	0.370	145.906 (μH)	47.502 (μH)	30.803 (μH)	81.4
4 cm	0.306	143.277 (μH)	46.692 (μH)	25.124 (μH)	69.5
6 cm	0.255	141.833 (μH)	46.235 (μH)	20.707 (μH)	56.2
8 cm	0.213	140.895 (μH)	45.928 (μH)	17.214 (μH)	43.2
10 cm	0.179	140.446 (μH)	45.776 (μH)	14.402 (μH)	30.1

Table 6. k, M and efficiency values calculated according to aligned state

Type 1		0 cm	2 cm	4 cm	6 cm	8 cm	10 cm
k	ANSYS	0.300	0.253	0.214	0.182	0.154	0.133
	Matlab (WHA)	0.318	0.261	0.278	0.194	0.159	0.141
M (μH)	ANSYS	13.441	11.562	9.911	8.502	7.301	6.286

	Matlab (WHA)	13.524	11.602	10.096	8.589	7.324	6.308
Efficiency (%)	ANSYS	80.4	76.1	70.9	51.3	39.2	24.5
	Matlab (WHA)	81.5	76.9	71.7	51.9	40.6	25.3
Type 2							
k	ANSYS	0.469	0.384	0.312	0.269	0.218	0.181
	Matlab (WHA)	0.498	0.397	0.324	0.278	0.227	0.189
M (μH)	ANSYS	38.654	31.178	25.340	20.881	17.352	14.515
	Matlab (WHA)	39.034	32.026	25.670	21.006	17.458	14.678
Efficiency (%)	ANSYS	88.3	84.2	73.1	59.6	45.2	31.8
	Matlab (WHA)	89.2	85.4	74.6	60.9	46.9	32.7
Type 3							
k	ANSYS	0.448	0.370	0.306	0.255	0.213	0.179
	Matlab (WHA)	0.512	0.384	0.32	0.265	0.221	0.186
M (μH)	ANSYS	38.266	30.803	25.124	20.707	17.214	14.402
	Matlab (WHA)	38.996	31.234	25.345	20.896	17.456	14.658
Efficiency (%)	ANSYS	86.3	81.4	69.5	56.2	43.2	30.1
	Matlab (WHA)	87.1	82.2	70.7	57.3	44.2	30.9

Table 7- Analysis results of unaligned coils of Type 1 WPT transformer

Distance	Coupling coefficient (k)	Transmitter coil inductance (L_p)	Receiver coil inductance (L_s)	Mutual inductance (M)	Efficiency (%)
0 cm	0.301	78.196 (μH)	25.543 (μH)	13.440 (μH)	79.8
2 cm	0.296	78.264 (μH)	25.558 (μH)	13.274 (μH)	75.7
4 cm	0.285	78.324 (μH)	25.561 (μH)	12.784 (μH)	69.8
6 cm	0.268	78.213 (μH)	25.567 (μH)	11.996 (μH)	49.3
8 cm	0.246	78.257 (μH)	25.586 (μH)	11.008 (μH)	38.2
10 cm	0.220	78.319 (μH)	26.567 (μH)	9.881 (μH)	23.9

Table 8- Analysis results of unaligned coils of type 2 WPT transformer

Distance	Coupling coefficient (k)	Transmitter coil inductance (L_p)	Receiver coil inductance (L_s)	Mutual inductance (M)	Efficiency (%)
0 cm	0.449	150.066 (μH)	49.051 (μH)	38.607 (μH)	87.9
2 cm	0.442	150.611 (μH)	49.126 (μH)	38.105 (μH)	83.8
4 cm	0.423	150.531 (μH)	49.151 (μH)	36.388 (μH)	72.2
6 cm	0.392	150.764 (μH)	49.251 (μH)	33.806 (μH)	58.7
8 cm	0.354	151.093 (μH)	49.329 (μH)	30.576 (μH)	44.1
10 cm	0.311	151.292 (μH)	49.423 (μH)	26.925 (μH)	30.8

Table 9- Analysis results of unaligned coils of Type 3 WPT transformer

Distance	Coupling coefficient (k)	Transmitter coil inductance (L_p)	Receiver coil inductance (L_s)	Mutual inductance (M)	Efficiency (%)
0 cm	0.447	148.699 (μH)	48.526 (μH)	38.055 (μH)	85.7
2 cm	0.441	148.686 (μH)	48.619 (μH)	37.506 (μH)	80.4
4 cm	0.421	148.813 (μH)	48.696 (μH)	35.856 (μH)	68.6
6 cm	0.390	149.060 (μH)	48.768 (μH)	33.334 (μH)	55.8
8 cm	0.353	149.273 (μH)	48.847 (μH)	30.147 (μH)	42.1
10 cm	0.310	149.637 (μH)	48.941 (μH)	26.560 (μH)	29.3

Tablo 10. k, M and efficiency values calculated according to unaligned coils

Type 1		**0 cm**	**2 cm**	**4 cm**	**6 cm**	**8 cm**	**10 cm**
k	ANSYS	0.301	0.296	0.285	0.268	0.246	0.220
	Matlab (WHA)	0.321	0.308	0.298	0.282	0.256	0.29
M (μH)	ANSYS	13.440	13.274	12.784	11.996	11.008	9.881
	Matlab (WHA)	13.943	13.580	12.980	12.098	11.178	9.997
Efficiency (%)	ANSYS	79.8	75.7	69.8	49.3	38.2	23.9
	Matlab (WHA)	80.6	76.8	71	50.9	39.2	24.6
Type 2							
k	ANSYS	0.449	0.442	0.423	0.392	0.354	0.311
	Matlab (WHA)	0.486	0.476	0.451	0.412	0.378	0.328
M	ANSYS	38.607	38.105	36.388	33.806	30.576	26.925
	Matlab (WHA)	39.056	38.452	36.534	34.098	30.868	27.124
Efficiency (%)	ANSYS	87.9	83.8	72.2	58.7	44.1	30.8
	Matlab (WHA)	89.1	84.9	73	59.6	44.8	31.4
Type 3							
k	ANSYS	0.447	0.441	0.421	0.390	0.353	0.310
	Matlab (WHA)	0.492	0.478	0.456	0.418	0.377	0.326
M	ANSYS	38.055	37.506	35.856	33.334	30.147	26.560
	Matlab (WHA)	38.707	38.096	36.368	33.880	30.452	26.968
Efficiency (%)	ANSYS	85.7	80.4	68.6	55.8	42.1	29.3
	Matlab (WHA)	86.9	81.2	70.1	56.7	42.8	29.8

Biography

Yıldırım Özüpak was born in 1985 in Muş. He received his bachelor's degree in Electronic Engineering from Inonu University in 2011. He received his MSc and PhD degrees in electrical and electronics engineering from Inonu University. His current research interests include wireless energy transfer, design of electric motors, machine learning and deep learning.

Mehmet Çınar was born in Elazığ. He received his bachelor's degree in Electrical Engineering from Istanbul Technical University. He received his PhD degrees in electrical and electronics engineering from Inonu University. His current interests include control and automation.